Surface finish of Additively Manufactured Metals: biofilm formation and cellular attachment

Paola Ginestra, Leonardo Riva, Elisabetta Ceretti, David Lobo, Sophie Mountcastle, Victor Villapun, Sophie Cox, Liam Grover, Moataz Attallah, Owen Addison, Duncan Shepherd and Mark Webber

Paola Ginestra. Department of Mechanical and Industrial Engineering, University of Brescia, Via Branze 38, 25123 Brescia, Italy
Corresponding author: paola.ginestra@unibs.it

Leonardo Riva. Department of Mechanical and Industrial Engineering, University of Brescia, Via Branze 38, 25123 Brescia, Italy

Elisabetta Ceretti. Department of Mechanical and Industrial Engineering, University of Brescia, Via Branze 38, 25123 Brescia, Italy

David Lobo. Department of Mechanical and Industrial Engineering, University of Brescia, Via Branze 38, 25123 Brescia, Italy

Sophie Mountcastle. School of Chemical Engineering, University of Birmingham, Edgbaston, Birmingham B15 2TT, UK

Victor Villapun. School of Chemical Engineering, University of Birmingham, Edgbaston, Birmingham B15 2TT, UK

Sophie Cox. School of Chemical Engineering, University of Birmingham, Edgbaston, Birmingham B15 2TT, UK

Liam Grover. School of Chemical Engineering, University of Birmingham, Edgbaston, Birmingham B15 2TT, UK

Moataz Attallah. School of Metallurgy and Materials, University of Birmingham, Edgbaston, Birmingham B15 2TT, UK

Owen Addison. School of Dentistry, University of Birmingham, 5 Mill Pool Way, Edgbaston, Birmingham B5 7EG, UK

Duncan Shepherd. Department of Mechanical Engineering, University of Birmingham, 5 Mill Pool Way, Edgbaston, Birmingham B5 7EG, UK

Mark Webber. School of Biosciences, University of Birmingham, Edgbaston, Birmingham B15 2TT, UK

Abstract. Powder bed fusion techniques enable the production of customized and complex devices that meet the requirements of the end user and target application. The medical industry relies on these additive manufacturing technologies for the advantages that these methods offer to accurately fit the patients' needs. Besides the recent improvements, the production process of 3D printed bespoke implants still requires optimization to achieve the optimal properties that can mimic both the chemical and mechanical characteristics of the anatomical region of interest. In particular, the surface properties of an implant device are crucial to obtain a strong interface and connection with the physiological environment. The layer by layer manufacturing processes lead to the production of complex and high-performance substrates but always require surface treatments during post-processing to improve the implant interaction with the natural tissues and promote a shorter assimilation for the fast recovery and wellness of the patient. Although the surface finishing can be tailored to enhance cells adhesion, proliferation and differentiation in contact with a metal implant, the same surface properties can have a different outcome when dealing with bacteria. This work aims to provide a preliminary analysis on how different post-processing techniques have distinct effects on cells and bacteria colonization of 3D printed titanium implants. The goal of the paper is to highlight the importance of the identification of an optimized methodology for the surface treatment of Ti6Al4V samples produced by Selective Laser Melting (SLM) that improves the implant antimicrobial properties and promotes the osseointegration in a long-term period.

Keywords. Selective Laser Melting, Titanium, Finishing, Additive Manufacturing, Metals

1 Introduction

The demand for implantable devices is expected to rise consistently over the next two decades. Longer life expectancy and an increase in population will raise the volume of medical implantable devices, while the higher mobility demanded by younger patients may outliving such devices. This increase in demand is linked to the inherent complexity of the required implant which paired with the differences between patients makes difficult their standardization, originating the challenge to manufacture high quality and vastly different implantable devices to modern engineering [1,2]. Additive

manufacturing (AM) techniques allow the production of highly customized implants meeting the final application specifications. Powder bed fusion processes offer the possibility of fabrication of complex and bespoke metal parts usually characterized by scarce surface finishing [3]. The surface quality of 3D printed parts is extremely important for the biological outcomes of both cells and bacteria colonization during *in vivo* conditions [4,5]. Infection of implantable devices is, still today, a great healthcare concern. Each year 1 to 5 % indwelling prosthetics became infected [6] where an attempt of salvaging the prosthetics through debridement of the infected site and long term antibiotic treatment are preferred over replacement, but literature shows that this procedure success rates range can be as low as 30 to 50% [7,8,9]. Antimicrobial coatings, photocatalysis antibiodies and antibiotics can be applyed to titanium surfaces to add an active mechanism of defence against bacteria colonization [10], but they are time consuming and complicate the part processing and supply chain. Polishing, etching and sandblasting finishing are commercially available treatments implementable with relatively easy application [11]. Their low cost, practicality and simplicity make them ideal candidates to treat additive manufactured parts. Biofilm formation, cell adhesion and differentiation had been shown to be heavily influenced by the aforementioned treatments, with substantial increases in osteogenesis and hindering of biofilm formation. This demonstrates a real possibility of tailoring the healing response of an implantable device with simple post processing techniques, but optimization of both cell adhesion and biofilm hindering remains a challenge while its impact on untreated additive manufacturing parts its mostly unknown. In this paper, AM samples are produced by Selective Laser Melting (SLM) and the effect on bacterial and cells adhesion of post-processing techniques such as polishing, passivation and sandblasting followed by passivation are demonstrated.

2 Manufacturing and post processing

2.1 SLM samples fabrication and treatment

The Ti6Al4V (Ti64) atomized powder was fully characterized before processing as reported in [12]. Briefly, the morphology of the powder particles and particle size distribution have been analyzed to assess the homogeneity of the powder before the printing and the flow properties have been examined to verify the dynamic properties and consequently the flow ability under low stress conditions.

For this research, cubical samples of 10 mm^3 were printed with a M2 Cusing SLM system (Concept Laser, Germany). An island pattern was chosen and the parameters for the fabrication were set as: 20 μm layer thickness, 75 μm hatch spacing, 1750 mm/s scanning speed and 150 W laser power.

As fabricated (AF) parts were then processed by polishing (PO), passivation (PA) and sandblasting followed by passivation (SP). All the post-processing techniques were applied to both the top and the side surfaces of the specimens and selected as commonly used in industrial standard operations to modify the surface finish of as built parts. The polishing process was performed using a centrifugal disc finishing machine (Finishing Techniques Ltd., FINTEK) with multiple stages. The whole process was carried out firstly using a G240 grinding disk, then a G1200 and finally a G4000 grinding disk followed by a polishing cloth with aluminum oxide balls (6−10 mm) to deburr and polish the parts, with total process duration of 8 h. All parts were cleaned using compressed air, an ultrasonic bath, and isopropyl alcohol. Passivated samples were obtained by etching in NHO_3 for 30 minutes. Sandblasting was performed in an Air Blast cabinet (CBI Equipment Ltd., UK) for 2 min with a speed of 100 m/s as previously reported [12]. Sandblasted samples were also passivated afterwards. Both the top surface and the side surface have been treated and analyzed.

3 Microstructural and biological characterization

3.1 Surface characterization of the samples

Micrographs of Ti-6Al-4V specimens were obtained using a XL30 FEG environmental SEM (Philips, UK) at 20 kV. Energy-dispersive X-ray spectroscopy (EDS) was used to evaluate the presence of contaminants due to the post-processing. The surface roughness of the as built and treated parts was analyzed using a Bruker Contour GT-K 3D Optical Microscope at 20× magnification.

The chemical properties of the surfaces were characterized by measuring the contact angle (CA) using a Attension® Theta tensiometer (Biolin Scientific). A droplet of deionized water (5 µm) was pipetted onto the top and side surfaces of the samples. Three measurements of the roughness and contact angle were obtained on representative areas of the overall surface for three different sample variants.

3.2 Biological tests

Staphylococcus epidermidis (gram-positive) and Pseudomonas aeruginosa (gram-negative) were used to evaluate the adhesion of two bacterial strain on Ti64 surfaces as previously shown [12]. The crystal violet assay provided non spatially specific quantification of bacterial adhesion across the surfaces of the samples. Briefly, the samples were sterilized and 300µm of Lysogeny broth (LB - Sigma-Aldrich, UK), inoculated 1:100 of an overnight culture of Staphylococcus aureus and Pseudomonas aeruginosa was added. After incubation, the samples were removed from the media and then prepared for the SEM and for the crystal violet staining for bacteria quantification. The samples were then observed under Scanning Electron Microscopy (ZEISS, USA). Samples were then immersed in 1 mL of 1% (w/v) crystal violet (CV) solution for 10 min to bound the dye with the bacteria. Overnight cultures in LB were diluted to an optical density 600 nm. Three absorbance readings were obtained from each replicate using a FluoSTAR Optima plate reader (BMG Labtech).

Human osteosarcoma cells (SAOS-2) were cultured in a proliferation medium composed by McCoys media (Thermo Fisher Scientific) supplemented with 10% FCS (fetal calf serum) and 100 units/ml of pen/strep in a humidified incubator at 37°C and 5% CO2. The mineralization medium was prepared by adding 50 µg/ml ascorbic acid (Sigma-Aldrich, UK),10-8M dexamethasone (cell culture tested) (Sigma-Aldrich, UK) and 10 mM β-glycerophosphate (Sigma-Aldrich, UK) into the cell culture medium. Cultures are incubated for up to 21 days with media changes every 3 days initially then daily as the cells become more confluent.

4 Results

4.1 SEM and EDS results

Scanning electron micrographs of AF samples highlighted the presence of the island scanning as already reported [12].

Figure 1 reports the micrographs of the as fabricated and treated samples on both top and side surfaces.

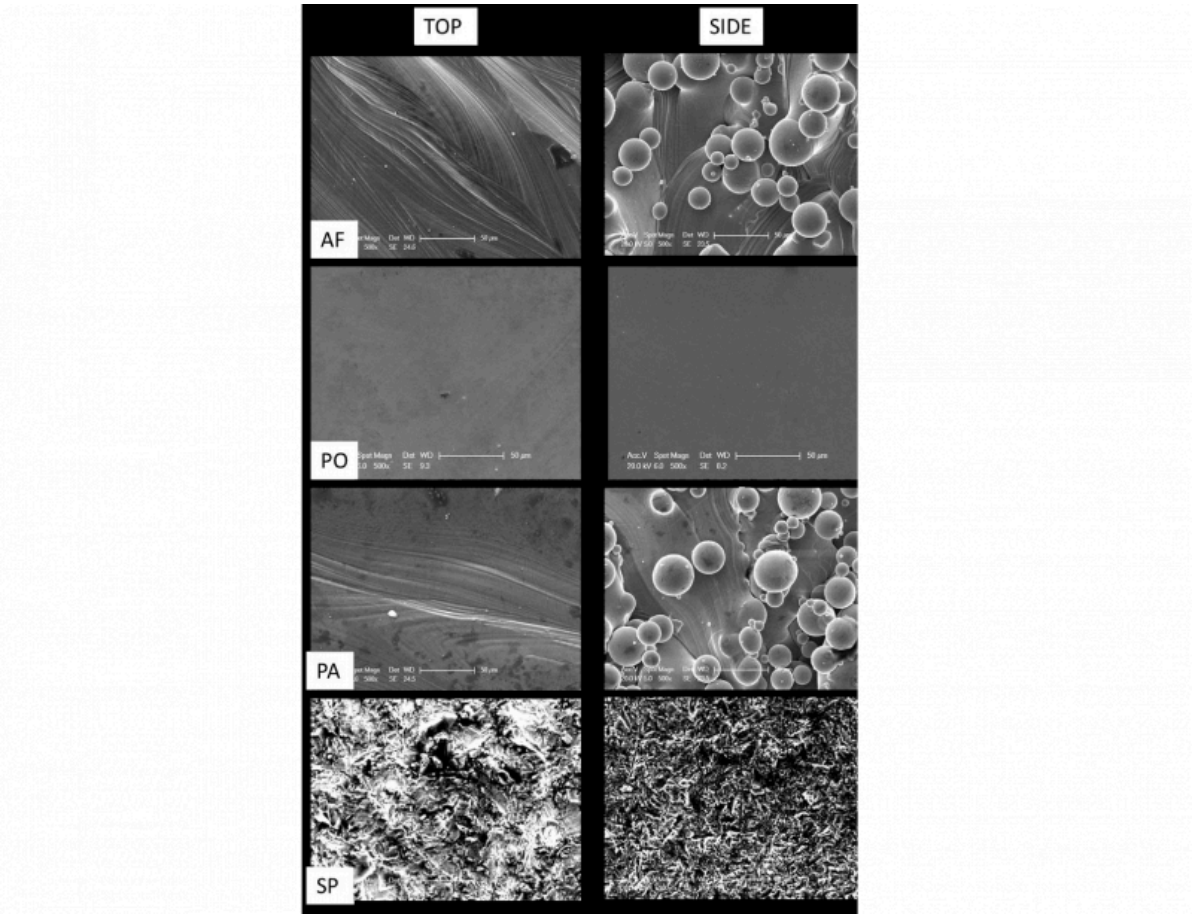

Fig. 1. SEM images of the top and side regions of as fabricated (AF), polished (PO), passivated (PA) and sandblasted and passivated (SP) samples. Scale bars are 50 µm

The laser track scans patterning are still visible on the top faces of the passivated samples while are not distinguishable anymore on the polished and sandblasted samples. No partially melted powder particles are observed after polishing while a greater number of partially melted particles are still visible on the passivated side face. The sandblasted samples report the presence of an irregular surface on both the top and the side surfaces as expected for the application of this treatment.

Table 1,2 and 3 show the chemical composition of the surfaces after the post processing treatments:

Table 1. Chemical composition of the Polished samples quantified from the EDS spectra

Polished					
Top			Side		
Element	Weight%	Atomic%	Element	Weight%	Atomic%
Al K	6.38	10.82	Al K	6.29	10.67
Ti K	89.62	85.59	Ti K	89.62	85.66
V K	4.00	3.59	V K	4.09	3.68

Table 2. Chemical composition of the Passivated samples quantified from the EDS spectra

Passivation					
Top			Side		
Element	Weight%	Atomic%	Element	Weight%	Atomic%
Al K	6.22	10.56	Al K	5.45	9.30
Ti K	89.85	85.91	Ti K	89.94	86.52
V K	3.92	3.53	V K	4.62	4.18

Table 3. Chemical composition of the Sandblasted and Passivated samples quantified from the EDS spectra

Sandblasted and Passivated					
Top			Side		
Element	Weight%	Atomic%	Element	Weight%	Atomic%
O K	6.72	16.1±1.7	O K	11.12	22.07±3.4
Al K	3.78	5.05	Al K	3.94	5.07
Si K	23.73	30.45	Si K	18.23	22.54
Ti K	63.11	47.48	Ti K	63.77	46.25
V K	2.66	1.88	V K	2.95	2.01

As expected, no contaminants are observed on polished and passivated samples while the sandblasting treatment leads to the presence of Si and oxygen. The Si presence is more evident on the top surface due to the possible presence of more adhesion sites for the contaminants while the oxidation level of the side surface is demonstrating a higher oxide layer resulting on the side face of the samples. In this case, the oxidation is not causing any presence of Fe on the treated samples.

4.2 Surface roughness results

The results of the roughness analysis on the surface of the samples are presented as mean and standard deviation of the mean (Fig. 2).

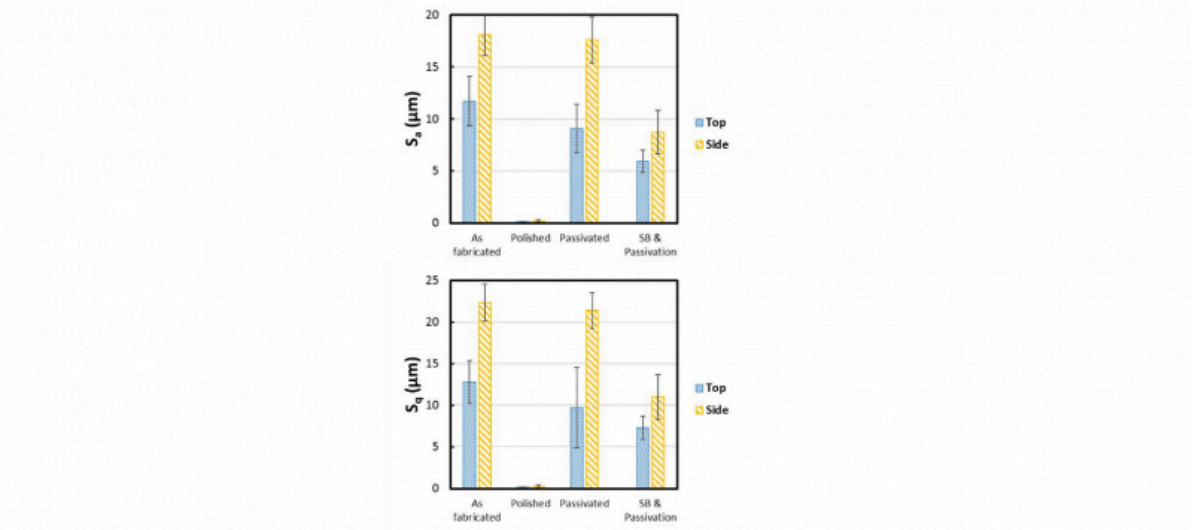

Fig. 2. Histograms of the Sa and Sq of the top and side faces of the as fabricated, polished, passivated and sandblasted and passivated samples

No significant difference between measurements of samples as fabricated and after passivation in relation to the Sa was

highlighted. The passivated samples demonstrated a slightly lower surface roughness in relation to the as fabricated on the top surface while on the side surface the surface topography is similar. Notably, the SP samples demonstrated a reduction of the surface roughness in relation to the AF on both top and side surfaces probably depending on the final quantity of partially un-melted powder on each sample. On the other hand, the polished samples reported an extremely low surface roughness on both top and side faces, as expected. The high variance of the data observed for all the post-processing techniques, excepting the polishing, demonstrated the inner stability of these processes. Generally, the lower values of roughness calculated for the top and side faces of the SP samples are highly related to the morphology of the surfaces after this treatment compared to the PA ones that is characterized with higher peaks similar to the AF surfaces.

4.3 Contact angle results

The contact angle of the top and side surfaces of the as fabricated and processed samples is reported in Figure 3 as mean and standard deviation of the mean.

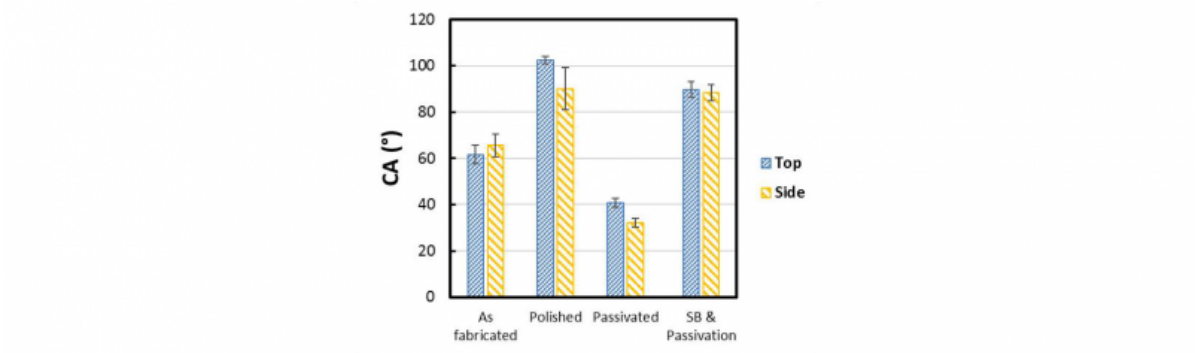

Fig. 3. Histograms of the CA of the top and side faces of the as fabricated, polished, passivated and sandblasted and passivated samples

Notably, the contact angle measurements on the top and side surfaces of the passivated samples are comparable and show substantially lower values in relation to the as fabricated parts. As expected, the polished samples report higher values of contact angles in relation to all the other samples especially in comparison with the passivated parts. It is interesting to highlight that the contact angle of the sandblasted samples is not lowered by the following passivation process.

Generally, the post processing treatments are increasing the contact angle of the surfaces enhancing the hydrophobicity of the faces with the exception of the passivated samples, as expected. The variability of the data observed for the side faces of the polished samples is probably due to the surface morphology of the as fabricated samples where an higher presence of spherical particles was reported.

4.4 Bacterial adhesion and staining

The S. epidermidis (Fig. 4) and P. aeruginosa (Fig. 5) images show the different adhesion of the bacterial strains on the as fabricated and treated samples.

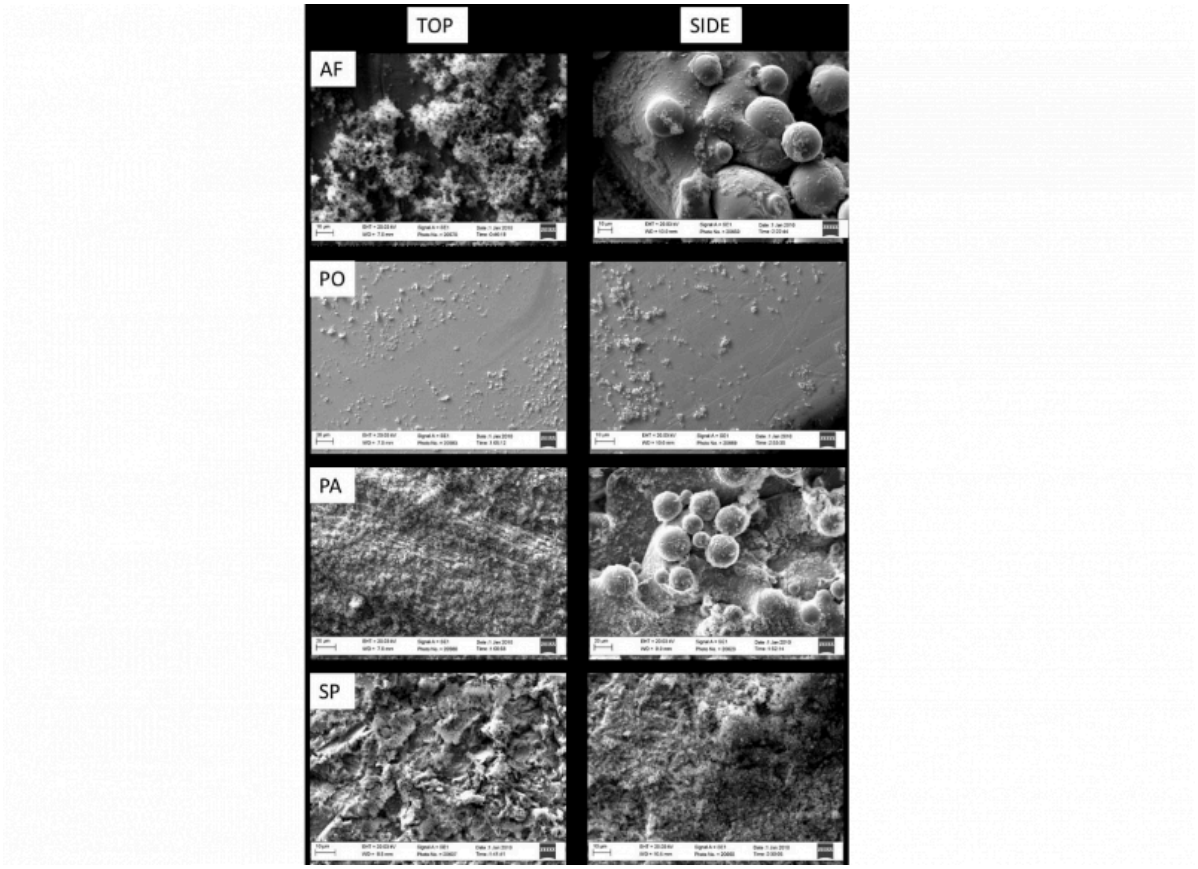

Fig. 4. SEM images of S. epidermidis biofilms formed on the top and side regions of AF, PO, PA and SP parts

As reported, the S. epidermidis is colonizing the as fabricated samples forming clumps especially on the top surface while on the side surfaces of both AF and PA samples, the bacteria are filling the gaps between the partially melted particles. On the top surface of the PA and SP samples instead, the S. epidermidis spreads onto the surface demonstrating that either the hydrophobicity or the topography of the surface can have a strong effect on the adhesion and proliferation of bacteria. On the other hand, despite the presence of fewer bacteria, it is notable a certain number of S. epidermidis on the top and side faces of the polished samples demonstrating that the treatment is effective in controlling the spreading of the bacteria preventing the formation of a biofilm in the short-term.

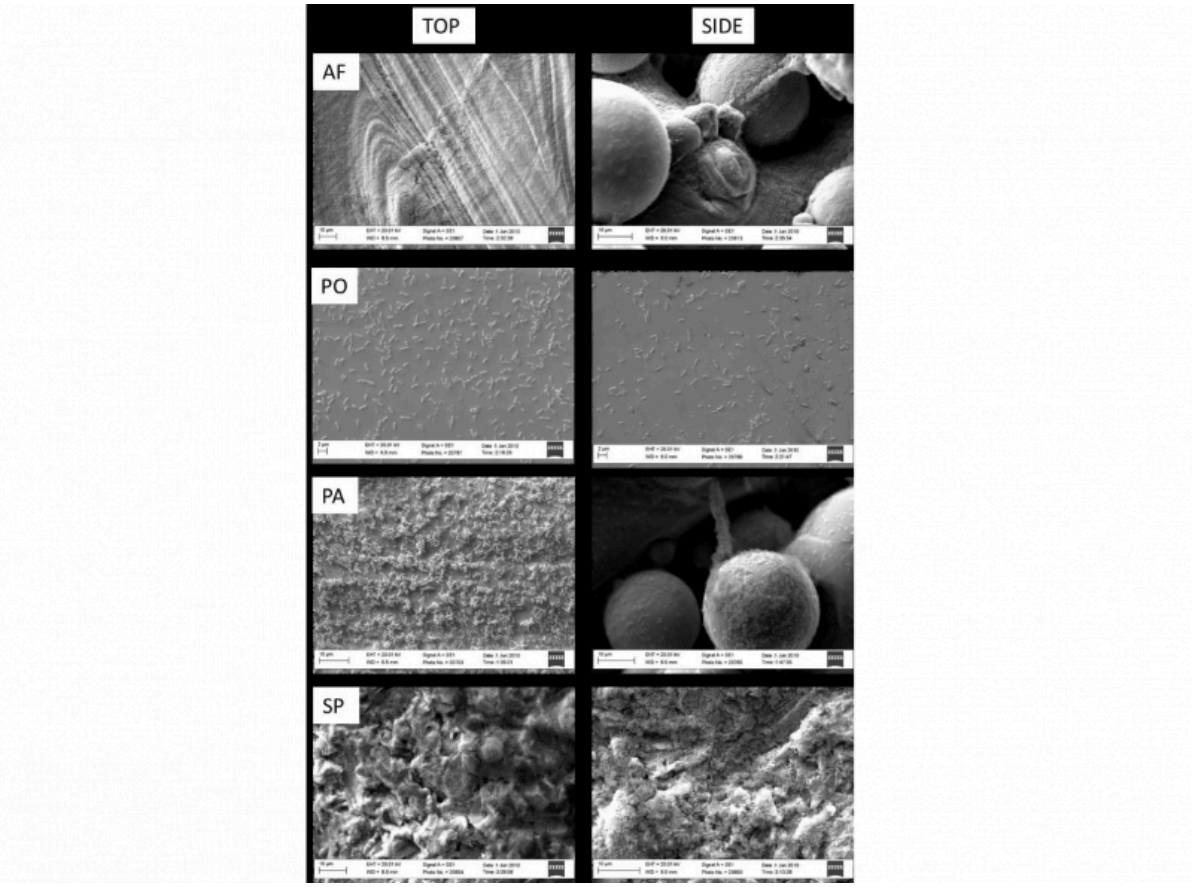

Fig. 5. SEM of P. aeruginosa biofilms formed on the top and side regions of AF, images PO, PA and SP parts

The P. aeruginosa spatial location on the AF top surface is similar to the SP ones due to the similar morphology of the two faces that allow the formation of a uniform layer of biofilm. The AF side surfaces show a similar trend of bacterial spreading compared to the SP side faces due to the presence of spherical particles that enable the communication of the gram negative bacteria from a unmelted powder to another. Notably, the spreading of bacteria on the top surface of PA samples seems disconnected and less homogeneous. As expected, on the polished surface no biofilm formation is visible unless the typical beam shape of the P. aeruginosa is still distinguishable due to the presence of few bacteria on the top and side surfaces.

The results of the Crystal violet staining are reported in Fig. 6.

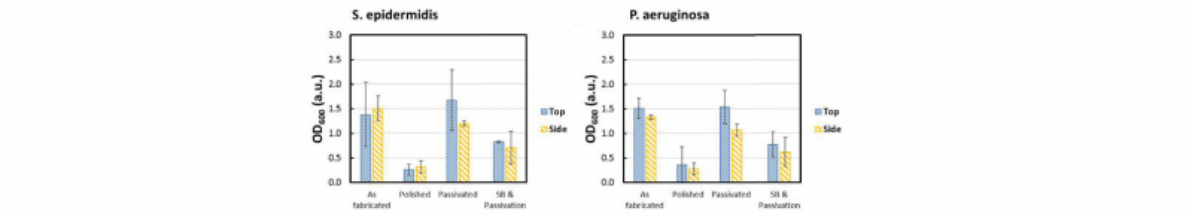

Fig. 6. CV absorption of S. epidermidis and P. aeruginosa bacteria on the AF, PO, PA and SP samples

The results show that the bacteria, both S. epidermidis and P. aeruginosa, are adhering on the different samples. In particular, the trends reported are confirming the impact of the surface roughness and contact angle of passivated samples on the bonding sites available for the bacteria to attach.

Notably, the staining shows that the bacteria are equally located on the top and side surface of the as fabricated and treated samples. Both strains quantifications show the lower level of colonization on PO samples while AF and PA report no significant difference on the bacteria presence. The quantitative results identify the PA samples as exposed as the AF ones to the bacterial colonization while the PO samples are the most effective against the microorganisms adhesion. The SP treatment is demonstrated to reduce the bacteria attachment in comparison with AF and PA samples.

4.5 Cells adhesion

The cells have been observed after 21 days of differentiation. The results are shown in Figure 7. As shown, the cells demonstrate to adhere on the top and side surfaces of all the analyzed samples. Notably, on the polished samples the cells are present in colonies with clusters caused by a limited mineralization of the cells. In this case, the differentiation of the cells has been compromised by the reduced adhesion due to the high hydrophobicity of the surface. The adhesion and mineralization of the osteoblasts seems to have the same trend on PA and SP samples. In particular, the chemical difference of the surfaces causes a more uniform spreading and thus the presence of scattered mineralization areas on the SP samples while the cells seem to be organized in agglomerations on the PA samples, especially on the side face. This trend is probably induced by the high roughness of the surface related to an enhanced hydrophilicity. Notably, the cells are spreading on the top and side surfaces of the AF samples with the formation of connected clumps on the side surface surrounding the spherical particles. In this case, the proliferation of the cells and the mineralization sites are less visible in comparison with the PA and SP treated samples.

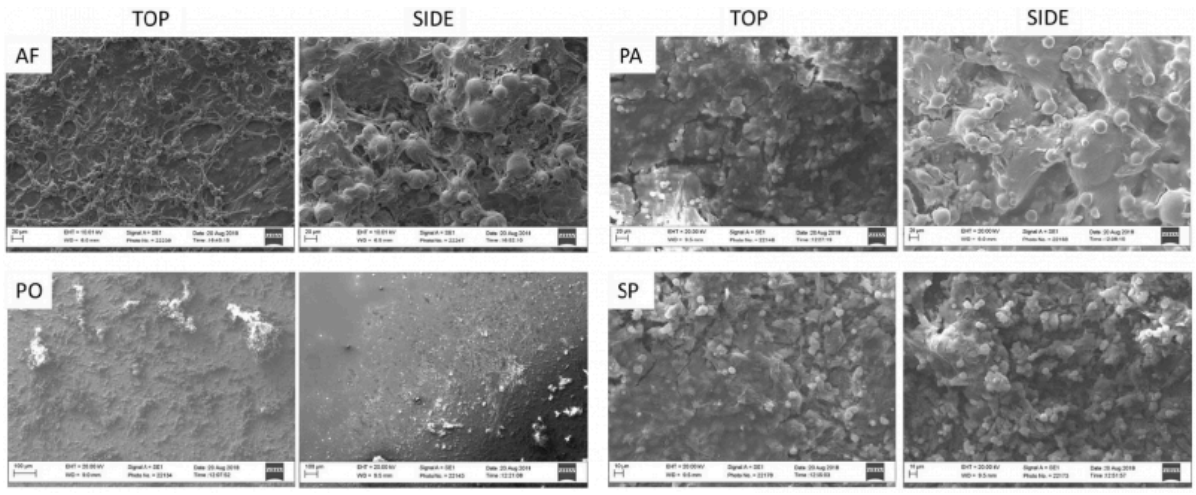

Figure 7. SEM images of SAOS-2 cells on the top and side regions of AF, PA, PO and SP samples. Scale bars are 20 μm for the AF, PA; 10μm for SP and 100μm for PO samples. The white spots visible on the micrographs are indicating the presence of mineralized areas

5 Discussion

The powder bed fusion processes allow the production of complex samples with bespoke properties but usually result in inadequate surface quality that can prevent the osseointegration of the parts. Typically, these manufacturing

technologies are followed by one or more post-processing of the samples to modify the surface finishing and meet the application requirements. This research demonstrated how specific treatments of the samples surfaces result in different outcomes in terms of chemical and topographical properties of the processed parts. The main effect of each treatment is related to the modification induced on the scanning track of the top surface and on the partially melted particles characterizing the side face of SLM samples.

The roughness of the surfaces has been modified more effectively with polishing and sandblasting while the final roughness of the passivated samples is demonstrated very similar to the roughness values measured for the as fabricated parts. On the other hand, the hydrophobicity of the samples has been deeply increased by the polishing process while the treatment that generated hydrophilic surfaces in relation to the as fabricated ones was the etching followed by the passivation of the metal samples. Notably, the sandblasting followed by passivation decreased the roughness of the samples especially on the side surface, confirming the uniformity of the surface with the majority of partially melted particles reached by the sandblasting. Contrarily, the passivation of the surfaces obtained after sandblasting did not cause a strong effect on the contact angle of the treated surfaces that resulted more hydrophobic than the as fabricated ones. This effect demonstrated that, despite the passivated samples resulted more hydrophilic than the as fabricated ones, when the passivation is combined with sandblasting, the samples are still showing higher contact angle in relation to the passivated surfaces. As expected, the polished surfaces resulted more hydrophobic not only compared to the as fabricated but also to the PA and SP surfaces. The sandblasting and polishing treatment introduced an increased uniformity between the top and the side faces of the samples, reducing the impact of the metal particles on the side surface. Differently, the passivation process resulted in a visible difference between the roughness of the top and the side surfaces, as reported for the fabricated specimens, while this distinction is less evident on the contact angle analysis due to the chemical changes introduced on the samples. The chemistry and topography of the surfaces are reflected on the biological results. In particular, the used bacterial strains showed the formation of a spreading biofilm on all the samples except for the polished ones where the number of microorganism is undoubtedly lower. The presence of spherical particles on the side surfaces of as fabricated and passivated is causing the formation of uncontrollable adhesion sites that would make these samples difficult to treat in case of infection. Furthermore, the sandblasted samples, despite showing a uniform spread of both the gram positive and gram negative bacteria, exhibited a proper adhesion and mineralization of the cells. The passivated surfaces instead, showed the adhesion and partial mineralization of cells in agglomerated state as on the as fabricated samples. As expected, the polished surfaces prevented the attachment of a proper amount of cells that result isolated and unable to properly colonize the samples. The same behavior was shown by the bacteria on the polished surfaces that prevented the formation of a homogenous biofilm.

6 Conclusions

The paper reports the effects on bacteria and cells adhesion of modifying the surface chemistry and topography of additively manufactured implants by the most used postprocessing processes: polishing, etching and sandblasting. The presented approach offers the opportunity to analyze the differences of antimicrobial and osseointegration properties of 3D printed implants for orthopedic applications. This work highlighted the necessity of minimizing the presence of particles on Ti6Al4V SLM specimens that could prevent a proper adhesion of the cells and promote the S. epidermidis and P. aeruginosa colonization of the surfaces. The polishing treatment of the parts, typically performed on parts before implantation, has been demonstrated effective for reducing the bacterial presence. Although, the presented preliminary study on cell adhesion and mineralization showed that surface polishing can impede the attachment of the cells.

The proposed methodology highlights the necessity of combining physical, chemical and mechanical approaches to properly promote osseointegration reducing the effect of a short-term bacterial infection.

Acknowledgements

The authors would like to acknowledge the grants EP/P02341X/1 (PREVENTION) and OPTIMIB for funding this research.

Bibliography

[1] Gastaldi D, Parisi G, Lucchini R, Contro R, Bignozzi S, Ginestra PS, Filardo G, Kon E, Vena P. A predictive model for the elastic properties of a collagen-hydroxyapatite porous scaffold for multi-layer osteochondral substitutes. 2015; 7(4): 1550063.

[2] Ginestra P, Ceretti E, Fiorentino A. Potential of modeling and simulations of bioengineered devices: enfoprostheses, prostheses and orthoses. Proceedings of the Institution of Mechanical Engineers Part H Journal of Engineering in Medicine 2016; 230 (7).

[3] Allegri G, Colpani A, Ginestra PS, Attanasio A. An experimental study on micro-milling of a medical grade Co-Cr-Mo alloy produced by selective laser melting. Materials 2019; 12 (13). Article number 2208.

[4] Ginestra P, Pandini S, Fiorentino A, Benzoni P, Dell'Era P, Ceretti E. Microstructured scaffold for cellular guided orientation : PCL electrospinning on laser ablated titanium collector. CIRP Journal of Manufacturing Science and Technology. 2017; 19: 147-157.

[5] Ginestra P, Fiorentino A, Ceretti E. Micro-structuring of titanium collectors by laser ablation technique: a novel approach to produce micro-patterned scaffolds for tissue engineering applications. Procedia Cirp 2017; 65: 19-24.

[6] Brouqui, P., Rousseau, M. C., Stein, A., Drancourt, M., & Raoult, D. Treatment of Pseudomonas aeruginosa-infected orthopedic prostheses with ceftazidime-ciprofloxacin antibiotic combination. Antimicrobial agents and chemotherapy. 1995; 39(11), 2423-2425.

[7] Moran, E., Masters, S., Berendt, A. R., McLardy-Smith, P., Byren, I., & Atkins, B. L. Guiding empirical antibiotic therapy in orthopaedics: the microbiology of prosthetic joint infection managed by debridement, irrigation and prosthesis retention. Journal of Infection. 2007; 55(1), 1-7.

[8] Hsieh, P. H., Lee, M. S., Hsu, K. Y., Chang, Y. H., Shih, H. N., & Ueng, S. W. Gram-negative prosthetic joint infections: risk factors and outcome of treatment. Clinical Infectious Diseases. 2009; 49(7), 1036-1043.

[9] Uækay, I., & Bernard, L. Gram-negative versus gram-positive prosthetic joint infections. Clinical infectious diseases. 2010; 50(5), 795-795.

[10] Janson, O., Gururaj, S., Pujari-Palmer, S., Ott, M. K., Strømme, M., Engqvist, H., & Welch, K. Titanium surface modification to enhance antibacterial and bioactive properties while retaining biocompatibility. Materials Science and Engineering: C. 2019; 96, 272-279.

[11] Cox SC, Jamshidi P, Eisenstein NM, Webber MA, Burton H, Moakes RJ, Grover LM. Surface finish has a critical influence on biofilm formation and mammalian cell attachment to additively manufactured prosthetics. ACS Biomaterials Science & Engineering 2017; 3(8): 1616-1626.

[12] Ginestra, P., Ceretti, E., Lobo, D., Lowther, M., Cruchley, S., Kuehne, S., Villapun, V., Cox, S., Grover, L., Shepherd, D., Attallah, M., Addison, O., Webber, M. Post processing of 3D printed metal scaffolds: A preliminary study of antimicrobial efficiency. Procedia Manufacturing 2020; 47, pp. 1106-1112.